

Jack-Up Footing Penetration and Fixity Analyses

L. Kellezi

GEO – Danish Geotechnical Institute, Lyngby, Denmark

H. W. L. Hofstede

Marine Structure Consultants bv, Schiedam, The Netherlands

P. B. Hansen

GEO – Danish Geotechnical Institute, Lyngby, Denmark

ABSTRACT: For a jack-up rig structure to be located in the North Sea a practical methodology for footing-soil interaction analysis considering the installation and the operation phases is described. The soil conditions at the location consist of sand underlain by soft clay followed by sand and stiff clay. Penetration analyses are carried out for the skirted footing without/with application of suction. Most Probable (MP) and Highest Expected (HE) skirt resistances are calculated. For the operation phase footing stability and ultimate capacities under storm load conditions are assessed. 2D finite element (FE) modelling is applied as an alternative to the 3D one. The pore pressure increase for dynamic/cyclic (DC) loading is implemented from the critical suction value. For lower/upper bound soil parameters, the footing capacities and stiffness are checked for the given factored load paths. The yield envelopes for V-M (H-constant) and V-H (M = 0) are calculated. The horizontal, vertical and the rotational stiffness are derived applicable to structure analysis.

1 INTRODUCTION

Footing-soil interaction analysis is carried out as part of the design of a three-leg jack up rig structure to be installed at the proximity of an oil platform in the North Sea. The purpose of the analysis is to determine strength and stiffness capacities of the jack-up footings during installation (penetration) and operation (fixity), respectively. The analysis is based on SNAME (2002).

From the preliminary design the footing has diameter $D = 16$ m. From the jack-up structure design preload capabilities and the combined quasi-static (QS) (wind and current) and dynamic/cyclic (DC) (due to wave and jack-up dynamic behaviour) loads at three headings, are calculated.

Using the available soil data design soil profiles are established. For the installation phase conventional footing penetration, including application of a suction system, is calculated. For the elevated conditions maximum load capacities at yield, and foundation stiffness are derived. The stability of the foundation is checked for the applied loads. Similar research is carried out from Bransby & Randolph (1999), Gourvenec (2003).

2 FOOTING GEOMETRY

The jack-up footing is constructed from a spudcan body and grout boxes installed around it. To improve footing stability and to serve as a mean for scour protection, an outer steel skirt is mounted around the perimeter of the grout boxes. The dimension outer skirt/spudcan tip to the largest contact footing area is about 3.0 m. The footing is not

equipped with dowels. Brackets are installed to reinforce the outer skirt. Inner skirts, (diaphragms or ribs), divide in compartments the volume between the spudcan, grout boxes and the outer skirt.

The footing concept design is shown in Figure 1.

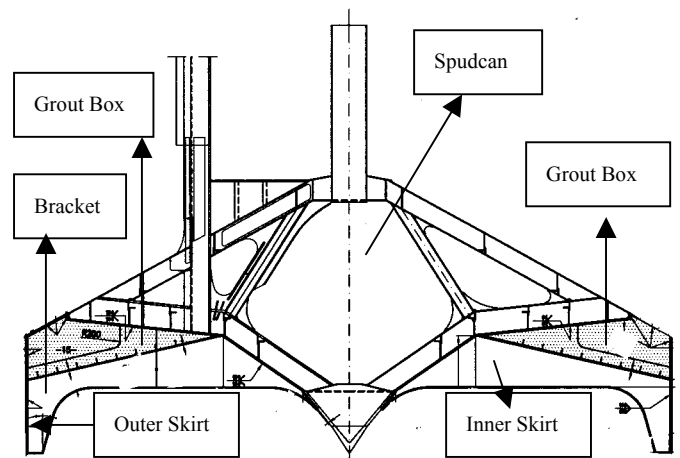


Figure 1. Footing cross section view

3 SOIL CONDITIONS AND WATER DEPTH

The geology at the location is characterized by layers of Pleistocene and Holocene age. The site investigation consists of four boreholes/CPT (cone penetration tests) to 20 m depth, one composite CPT and sampling borehole to 80 m depth and offshore, on-shore laboratory testing. The water depth is 44 m.

The data are used to derive the designed soil profile at the location, consisting of sand layers underlain by soft clay, followed by sand and stiff glacio-marine clay to the depth applicable to foundation analyses. Lower/upper bound design soil profiles

and parameters are given in Table 1. In such assessments the characteristic parameters have been selected as a cautious estimate of the value effecting the occurrence of the relevant limit state, Eurocode 7 (1997).

Drained loading conditions are considered for the sand layers and undrained for the clay layers. The design friction angles have been evaluated from relative densities interpreted from CPT data and drained triaxial test results. The design undrained shear strength values are mainly evaluated from the unconsolidated undrained (UU) and consolidated undrained (CIU) triaxial and field laboratory (torvane and penetrometer) tests.

Table 1. Lower/upper bound design soil profile

Soil Type	Depth of Layer (m)		Unit Weight γ' (kN/m ³)	Angle of Internal Friction ϕ (°)		Undrained Shear Strength c_u (kN/m ²)	
	Top	Bottom		Lower Bound	Upper Bound	Lower Bound	Upper Bound
	SAND, silty fine, very loose to medium dense	0		0.9	8	25	30
SAND, silty fine, dense to very dense	0.9	3.5	10	35	40	-	-
CLAY, very soft to soft	3.5	5.0	6	-	-	15	25
SAND, silty fine, medium dense to dense	5.0	6.0	9	30	35	-	-
CLAY, firm to very stiff	6.0	20	10	-	-	$60+4*d$	$60+8*d$

d denotes the depth below the soft clay layer

4 INSTALLATION PHASE, CONVENTIONAL PENETRATION ANALYSIS

To define footing penetration depth for the maximum preload assessment of the static bearing capacity of the spudcan in combination with the grout boxes and the skirt, at various depths, is carried out.

4.1 Penetration analysis, no suction applied

The footing bearing capacity is calculated mainly based on Hansen (1970) and authors experience with spudcan penetration prediction in the North Sea, Kellezi & Stromann (2003). The spudcan body and the grout boxes are simplified to an equivalent circular footing with a flat bottom.

The derived lower/upper bound design soil profiles are applied in the conventional penetration analysis. As sand overlies soft clay punching failure is investigated using a load spread assumption of 1:3. Firstly, the penetration of the spudcan tip in the sand layer occurs. Next, squeezing of the soft clay is initiated and developed.

The penetration resistance of the skirt elements is the sum of skin resistance and the end resistance. Two calculations, respectively Most Probable (MP) and Highest Expected (HE) are carried out based on DNV (1992). The latter governs the requirements to

the penetration force. The calculation of the skirt resistance is based on the CPT data, which give a continuous record of the cone resistance with depth. For the chosen CPT's an average cone resistance at 0.2 m interval is calculated.

Skirt resistance is calculated as a function of average cone resistance q_c and empirical coefficients k_p and k_f , which relates q_c to skirt end resistance and skin friction. In the current analysis, $k_p = 0.3$ and $k_f = 0.001$ are chosen for the sand layers when calculating the MP resistance and $k_p = 0.6$ and $k_f = 0.003$ for HE resistance. About 25% smaller values of these coefficients are applied in the upper first metre due to local piping or lateral structure movement.

Several uncertainties remain regarding the conversion from MP to HE resistance considering the effect of penetration rate and generation of the pore pressure during CPT testing. Therefore, a consistent set of correlation factors does not exist. Soil resistance versus penetration is given in Figure 2.

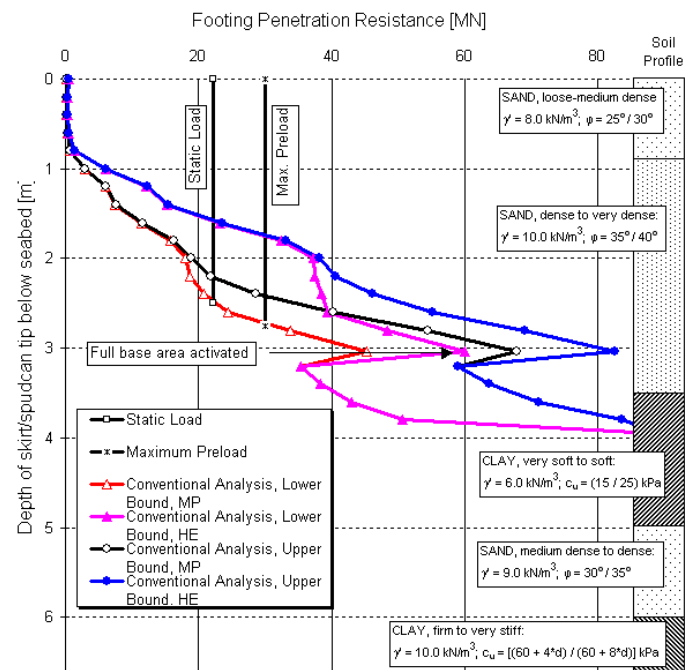


Figure 2. Footing penetration curves

The results show that there is a slight risk of punch through for vertical load larger than about 35 MN/leg and lower bound soil parameters. This can be associated with a sudden penetration of 0.5 m for MP skirt resistance and footing penetration of 2.75 m. For HE skirt resistance and footing penetration of 2.5 m, the sudden penetration can be 0.7 m. However, this load level is not reached in a storm condition.

4.2 Penetration analysis applying suction

For maximum preload of 30 MN/leg the skirt is not expected to fully penetrate into the dense to very dense sand layer, resulting in a penetration of 1.75 m for lower/upper bound soil data and HE skirt resistance.

The possibility of increasing the skirt penetration by applying suction is investigated before the installation phase. Initially, footing will penetrate during application of the maximum preload of 30 MN/leg. After this, subsequent suction might be applied to reach the desired depth.

The driving force consisting of the preload and the suction, which is applied in the available volume surrounded by spudcan/grout boxes, the inner skirt compartments and the sand soil filling the skirts, should be larger than the resistance from the soil.

The resistance force can be subdivided into skin friction acting on the inner, respectively the outer skirt, combined with the skirt tip resistance and spudcan/grout boxes bearing capacity. The resistance force is a function of the suction factors. The skin friction changes due to suction. The inside skin friction reduces, whereas the outside skin friction increases, Clausen & Tjelta, (1996). In addition, the tip resistance is reduced. The maximum reduction is obtained when critical suction value is reached.

In the current penetrability analysis the critical suction is calculated based upon approximate numerical steady state flow solutions with $H/D < 0.5$. Regarding the inside skin friction, if critical suction occurs, there will be soil plug uplift. For installation purposes it is required to have some free space between the footing or spudcan lid and the soil plug. The heave of the soil plug is observed in the calculations to be 4 to 5% of the skirt penetration depth.

0.15 for the outer skirt skin resistance and $r_i = 0.9$ for the inner skirt skin resistance. The required suction to reach a desired depth is calculated. The penetration depth as a function of differential skirt water pressure (suction) is given in Figure 3.

The results are interpreted in such a way that, if the footing will not penetrate more than 1.75 m for maximum preload the proposed required suction to reach for example 2.5 m penetration is 37 kPa, if LB soil data reveals. If UB soil data applies at the site, maximum 2.3 m footing penetration should be expected applying suction less than the critical value of 49 kPa.

5 OPERATION PHASE, FE FIXITY ANALYSIS

The analyses applicable to the operation phase consider the assessment of footing foundation strength and stiffness under storm load conditions. Regarding foundation stability three-dimensional (3D) finite element (FE) modelling of the footing and the surrounding soil employing coupled pore pressure/deformation elements under dynamic loads, would be the target.

Taking into account the soil conditions at the location, the complexity of the problem, the use of lower/upper bound soil profiles and the fact that sufficient safeties are found in the V-H plane, two-dimensional (2D) FE deformation analyses for static load paths are carried out as an engineering alternative.

Footing penetration of 2.75 m during the jack-up installation is probably most critical (closer to the soft clay layer) for the stability analysis. Therefore, the fixity analyses for lower/upper bound soil parameters is carried out for footing at this penetration depth. The analyses are performed with FE program Plaxis V8.2 (2002) applying updated mesh and Mohr Coulomb nonlinear soil constitutive model for sand and clay layers.

The soil strength parameters, as applied in the conventional penetration analysis are also implemented in the fixity FE model. In addition, in absence of laboratory data, dilatation angle $\psi = \phi - 30^\circ$ is derived. Other relationships such as $\psi = \phi$ and $\psi = \phi/2$ are also investigated.

The deformation parameters are evaluated based on the geotechnical data, but mostly on the author's experiences with FE modelling in the North Sea. $E = 200 \cdot c_u$ is calculated for the clay layers and $E = 4 \cdot q_c$ for the sand layers.

The 2D FE model can be found in Figure 4. The 3D footing geometry is adapted in the 2D analysis.

5.1 2D FE footing modelling

The original 3D footing configuration is considered circular with radius R . To model it in 2D the circular

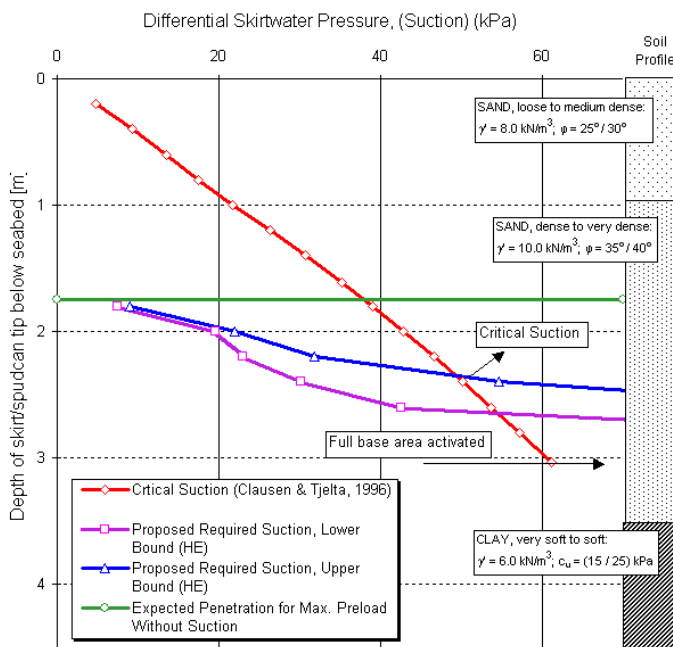


Figure 3. Footing penetrations versus suction

The outside skin friction is assumed to be increased by 10-15% for maximum suction, based on values reported from previous suction buckets installations in the North Sea.

A macro program is created to facilitate the current analyses. The reduction suction factors applied are $r_t = 0.1$ for the skirt/spudcan tip resistance, $r_o =$

The FE model is built asymmetric as asymmetric loads are applied. Standard boundary conditions are incorporated at the far field. The size of the model in the horizontal and the vertical direction is chosen so that the boundary conditions will not affect foundation capacity. The FE mesh is refined around the spudcan and is coarser far from it.

5.4 Suction during DC loads, critical suction

In the current 2D fixity analysis, where pseudo-static loads are applied, the suction effect is simulated from the critical suction concept based on calculated suction levels, giving exit gradients equal to one inside the skirt. This is compared directly to the measured differential pressure inside the skirted footing placed on frictional material in order to evaluate the state (safe/critical) of suction levels.

For large diameter footings such as the current one, a simple approach is to look upon the skirt tip as a sheet pile wall, Hansen (1978). A point of interest is the exit gradient, where the seeping water emerges behind the wall. The normalized critical suction is usually given as $u_{cr} = \pi * H * \gamma'$ where H is the outer skirt length. For $H/D < 0.5$, $u_{cr} = H * \gamma' / (1.0 - 0.68 / (1.46 * H/D + 1))$ is given by Clausen & Tjelta (1996) as used in section 4.2.

Critical suction is only valid for frictional materials. This applies to the soil profile at the considered location. When the critical suction is reached, a piping channel may start to form but this takes time, and short time suction higher than u_{cr} is therefore possible, even for fully drained conditions.

Based on the above, the suction effect is approximated in the 2D fixity analysis for DC LC by applying a distributed load equal to $u_{cr} = 3 * 2.75 * 9.1 = 75$ kPa at the level of outer skirt tip on the tension side of the footing as shown in Figure 4. The effective unit weight of the sand filling the skirt is taken as an average of the top sand layers. The width of the applied suction load is a function of the eccentricity value $e = M/V$ and is $2e = 1.69$ m for DC LC1, $2e = 3.63$ m for LC2 and $2e = 5.56$ m for LC3 considering the given load paths in Table 2 and the concept of the effective footing area.

5.5 Footing stability and ultimate capacity

Two scenarios, lower and upper bound soil parameters respectively, are considered in the current 2D FE analyses. For each scenario, the footing-soil system stability and stiffness are assessed for the given load paths and the ultimate limit state calculating the capacity at yield. The calculations are carried out as follows:

Stage 1: Load the footing with the maximum pre-load of 30 MN/leg (Plaxis staged construction). Stage 2: Unload to Static load. Stage 3: Apply the V-H-M for the QS LC1, LC2 and LC3. Stage 4: Apply

the H component from the DC load for the three LCs. Stage 5: Apply the V-M from the DC LCs. Stage 6: Apply the V-H from the DC LCs after Stage 2 checking the sliding capacity. Stage 7: Apply additional V-H loads increased by ratio after Stage 2, defining the ultimate V-H capacities. Stage 8: Apply additional V-M loads increased by ratio after Stage 4 to define the ultimate V-H-M capacities.

Table 3 V-H-M and V-H ultimate capacities, lower bound.

Lower Bound			V-H-M Capacity			V-H Capacity	
Load Comb	Angle (°)	Leg	V (MN)	H (MN)	M (MNm)	V (MN)	H (MN)
LC1	0	3	35.708	1.798	38.182	41.490	4.427
LC2	180	3	21.836	2.268	50.913	21.256	7.117
LC3	210	2	15.746	1.982	39.584	6.694	4.439

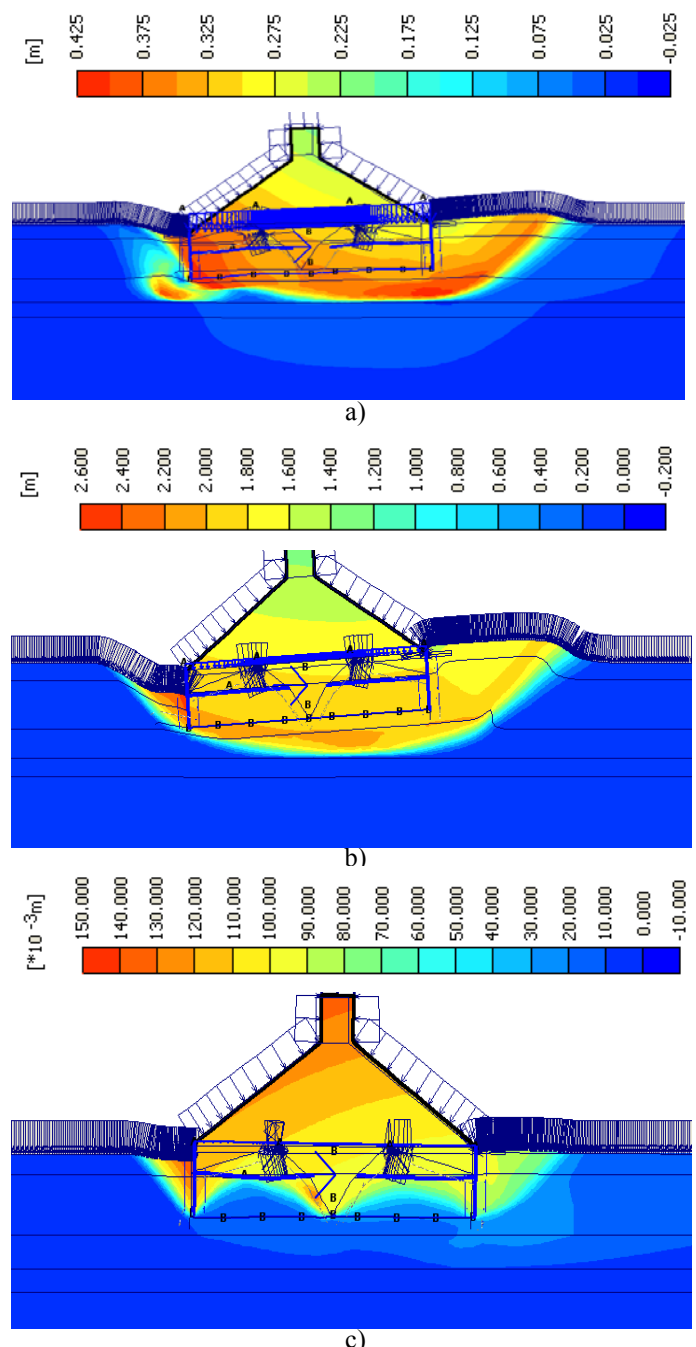


Figure 5. Sliding at yield. Total Displacements. a)LC1; b)LC2; c) LC3;

Except for the two first stages the rest are repeated for each load path. So in all, 20 stages are calculated for each scenario. The ultimate footing capacities (the load paths at yield) for lower bound soil parameters are given as 3D loads in Table 3.

They can be compared with the 3D load paths given in Table 2, showing that footing capacity for LC1 and LC2 is well satisfied (load vectors fall inside the yield surface) but LC3 is not completely satisfied for LB (load vectors fall in or slightly out of the yield surface). Safety in the V-H plane is checked. For UB conditions the ultimate capacity is larger than LC2. So LC2 is within the yield surface for this case. The results of the calculations are given in Figure 5 for the sliding and in Figure 6 for V-H-M ultimate capacities.

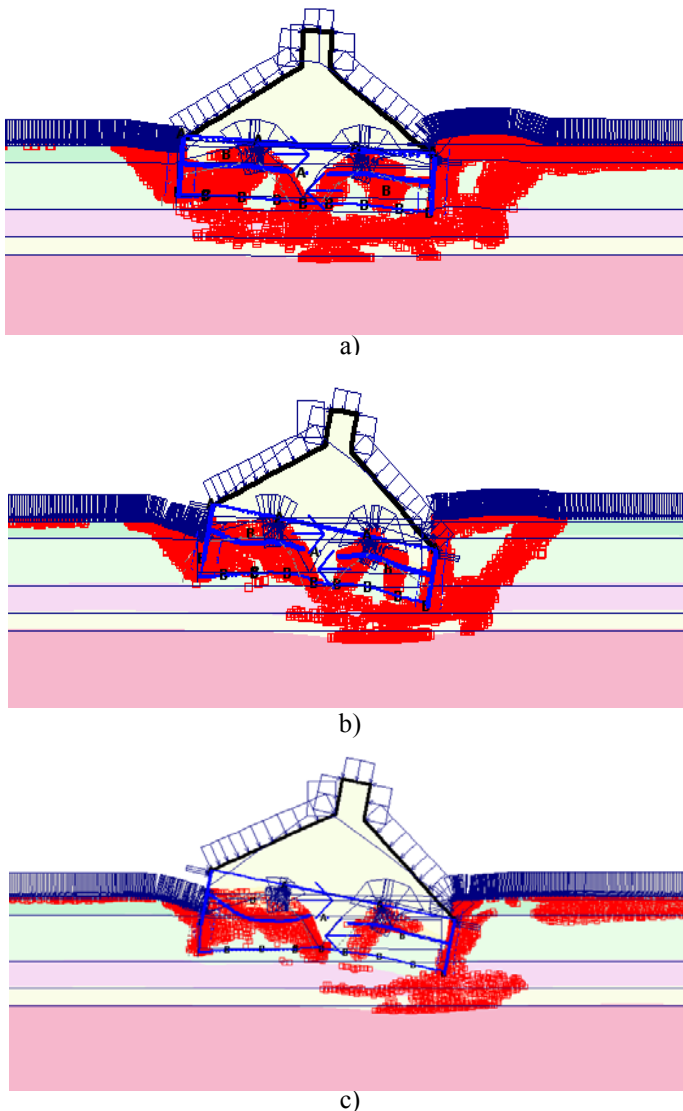


Figure 6. DC load at yield, rupture figures, a) LC1; b) LC2; c) LC3;

5.5.1 Investigated Failure Modes

Various failure modes are investigated for different LCs. Typical failure modes encountered are: Sliding at base with local failure around skirt tips, Figure 5a; Sliding along the soft clay layer below skirt tip, Figure 5a,b; Sliding along base of skirt tip, Figure 5c; Deep-seated failures governed by moment equilibrium with centre located anywhere, Fig-

ure 6a; Moment equilibrium centre below the foundation base, Figure 6b, c;

5.5.2 Footing-Soil Nonlinear Stiffness

The horizontal, vertical and the rotational stiffness for the footing are derived from the 2D fixity analyses. The rotation is derived based on the vertical stiffness for the left and the right points in the footing diameter. The failure loads are defined from the asymptote of the yield curves. This is taken into account when deriving the foundation stiffness for the structure analysis.

6 CONCLUSIONS

A methodology for a jack-up footing-soil interaction analyses is described. The installation and the operation phases are considered.

Penetrations analyses without/with application of suction are carried out calculating MP and HE skirt resistances. Fixity analyses consider the assessment of footing stability and ultimate capacity under storm load conditions. Suction effect during DC loading is implemented based on the critical suction concept. The horizontal, vertical and the rotational foundation capacities and stiffness are derived from the 2D fixity analyses found applicable and an effective engineering approximation.

REFERENCES

- Bransby M.F & Randolph M.F., 1999, The effect of skirted foundation shape on response to combined V-M-H loadings. *Int. Journal of Offshore and Polar Engineering*, (IJOPE) 9(3), page 214-218.
- Clausen C.J.F. & Tjelta T.L. 1996, Offshore Platforms Supported by Bucket Foundation. *Proc. 15th IABSE*, Copenhagen, page 819-829.
- DNV (Det Norske Veritas) 1992. *Foundations Classification Notes No. 30.4*. February.
- Eurocode 7, 1997, *Geotechnical Design, Part 1, General Rules*, CEN/TC 250, 2004-2009.
- Gourvenec S. 2003, Alternative design approach for skirted footings under general combined loading. *Proceed. of BGA International Conference on Foundations (ICOF)*, Dundee, 2-5 Sept. 2003, page 341-349.
- Hansen, J.B. 1970. A revised and extended formula for bearing capacity. *Bulletin No. 28*. The Danish Geotechnical Institute.
- Hansen B. 1978, *Geoteknik og Fundering del II*. Laboratoriet for fundering. Danmarks Tekniske Højskole (kursus 5821-geoteknik 2 (In Danish)).
- Kellezi, L. & Stromann H. 2003, FEM Analysis of Jack-up Spudcan Penetration for Multi-Layered Critical Soil Conditions. *Proc. of BGA Intern. Conf. on Foundations, ICOF2003*, Dundee, Scotland, 410-420.
- Plaxis V. 8.2 2002. *User Manual 2D*, Delft University Technology and Plaxis BV
- SNAME 2002. T&R Bulletin 5-5A. *Site Specific Assessment of Mobile Jack-Up Units*. The Society of Naval Architects and Marine Engineers.